The KASCADE-Grande experiment: measurements of the all-particle energy spectrum of cosmic rays

J.C. Arteaga-Velázquez,[1,*] W.D. Apel,[2] K. Bekk,[2] M. Bertaina,[3] J. Blümer,[2,1] H. Bozdog,[2] I.M. Brancus,[4] P. Buchholz,[5] E. Cantoni,[3,6] A. Chiavassa,[3] F. Cossavella,[1,†] K. Daumiller,[2] V. de Souza,[1,‡] F. Di Pierro,[3] P. Doll,[2] R. Engel,[2] J. Engler,[2] M. Finger,[2] D. Fuhrmann,[7] P.L. Ghia,[6] H.J. Gils,[2] R. Glasstetter,[7] C. Grupen,[5] A. Haungs,[2] D. Heck,[2] J.R. Hörandel,[1,§] T. Huege,[2] P.G. Isar,[2] K.-H. Kampert,[7] D. Kang,[1] D. Kickelbick,[5] H.O. Klages,[2] K. Link,[1] P. Łuczak,[8] M. Ludwig,[1] H.J. Mathes,[2] H.J. Mayer,[2] M. Melissas,[1] J. Milke,[2] B. Mitrica,[4] C. Morello,[6] G. Navarra,[3,¶] S. Nehls,[2] J. Oehlschläger,[2] S. Ostapchenko,[2,‖] S. Over,[5] N. Palmieri,[1] M. Petcu,[4] T. Pierog,[2] H. Rebel,[2] M. Roth,[2] H. Schieler,[2] F. Schröder,[2] O. Sima,[9] G. Toma,[4] G.C. Trinchero,[6] H. Ulrich,[2] A. Weindl,[2] J. Wochele,[2] M. Wommer,[2] and J. Zabierowski[8]

[1] *Institut für Experimentelle Kernphysik, Karlsruher Institut für Technologie - Campus Süd, Germany*
[2] *Institut für Kernphysik, Karlsruher Institut für Technologie - Campus Nord, Germany*
[3] *Dipartimento di Fisica Generale dell' Universita Torino, Italy*
[4] *National Institute of Physics and Nuclear Engineering, Bucharest, Romania*
[5] *Fachbereich Physik, Universität Siegen, Germany*
[6] *Istituto di Fisica dello Spazio Interplanetario, INAF Torino, Italy*
[7] *Fachbereich Physik, Universität Wuppertal, Germany*
[8] *Soltan Institute for Nuclear Studies, Lodz, Poland*
[9] *Department of Physics, University of Bucharest, Bucharest, Romania*

The all-particle energy spectrum as measured by the KASCADE-Grande experiment for $E = 10^{16} - 10^{18}$ eV is presented within the framework of the QGSJET II/FLUKA hadronic interaction models. Three different methods were applied based on the muon size and the total number of charged particles individually and in combination. From the study it is found that the spectrum cannot be completely described by a smooth power law due to the presence of characteristic features.

1. INTRODUCTION

Powerful cosmic ray accelerators are hidden inside our own galaxy and in the heart of extragalactic objects, but their precise location and exact working mechanism are still subject of intense debate. Cosmic ray research provides important clues through the measurement of the energy spectrum, the arrival direction and the composition of such enigmatic particles by means of the extensive air showers (EAS) that cosmic rays produce in the Earth atmosphere. Along the past years, dedicated experiments have shown that the energy spectrum of cosmic rays extends from a few MeV up to 10^{20} eV, has a striking power-law behavior with a spectral index $\gamma \approx -2.7$ and exhibits some intriguing structures around $3 - 5 \cdot 10^{15}$ and $4 - 10 \cdot 10^{18}$ eV, better known as the *knee* and the *ankle*, where the spectral index of the particle flux decreases and grows, respectively [1]. The precise interpretation of these features are not yet clear, but they could arise as a consequence of an interplay among different factors such as the loss of efficiency of the galactic accelerators, the dominance of a new component of extragalactic origin at the high-energy regime and the propagation effects of cosmic rays through space [2, 3]. To test different scenarios, accurate and high-statistics measurements are needed between 10^{15} and 10^{18} eV. Although observations of this kind have been already performed around the knee, the picture is not yet complete due to the lack of quality EAS data at higher energies: $E = 10^{16} - 10^{18}$ eV. The goal of the KASCADE-Grande experiment is to close this gap between the *knee* and the ultrahigh-energy region with accurate EAS measurements.

KASCADE-Grande is a ground-based EAS array integrated by different detection systems to measure and separate the muon and electromagnetic components of the EAS [4]. Once combined, both observables become a powerful tool to reconstruct the energy spectrum and to estimate the composition of primary cosmic ray events. In the following lines, the energy spectrum of cosmic rays for $E = 10^{16} - 10^{18}$ eV as measured by KASCADE-Grande will be presented and the reconstruction method will be described. First, a brief introduction to the characteristics and performance of the experiment will be given.

*corresponding author, email: arteaga@ifm.umich.mx; now at: Universidad Michoacana, Instituto de Física y Matemáticas, Mexico
†now at: Max-Planck-Institut für Physik, München, Germany
‡now at: Universidade São Paulo, Instituto de Física de São Carlos, Brasil
§now at: Dept. of Astrophysics, Radboud University Nijmegen, The Netherlands
¶deceased
‖now at: University of Trondheim, Norway

Table I: Some components of KASCADE-Grande: total sensitive areas and threshold kinematic energies for vertically incident particles are presented. MTD refers to the muon tracking detectors [4].

Detector	Particle	Area(m^2)	Threshold
Grande array (plastic scintillators)	Charged	370	3 MeV
Piccolo array (plastic scintillators)	Charged	80	3 MeV
KASCADE array (liquid scintillators)	e/γ	490	5 MeV
KASCADE array (shielded plast. scint.)	μ	622	230 MeV
MTD (streamer tubes)	μ	4×128	800 MeV

2. The KASCADE-Grande experiment

2.1. Description

The KASCADE-grande detector (located at 49.1° N, 8.4° E, 110 m a.s.l.) is the successor of the KASCADE experiment [5] and incorporates the original electromagnetic detectors and muon devices of KASCADE to a bigger system of detectors, called Grande, composed of a $700 \times 700\,m^2$ array with $37 \times 10\,m^2$ scintillator stations regularly spaced by an average distance of 137 m [4]. To coordinate the trigger of KASCADE with EAS events where the core is found inside Grande a smaller array, named Piccolo, was added. The main characteristics of the KASCADE-Grande detectors are displayed in table I and the layout of the experiment is presented in figure 1.

The Grande array is used to sample the density of charged particles of the shower front at ground level and to measure the particle arrival times of the EAS. The core position, the number of charged particles (N_{ch}) and the arrival direction of the shower are extracted from the Grande data through an iterative fit and a careful modeling of the EAS front. To reconstruct the arrival direction a χ^2 fit is applied assuming a curved shower front as suggested by CORSIKA/QGSJET II simulations. On the other hand, to obtain the core position and the shower size a maximum likelihood procedure was employed by using a modified NKG lateral distribution function as a reference model [4].

An important component of this experiment is the KASCADE muon array, composed by $192 \times 3.2\,m^2$ shielded scintillator detectors, which are sensitive to muons with threshold energy above 230 MeV for vertical incidence. With the Grande information and the measurements of the shielded array of the lateral distribution of muons in the shower front, the muon size (N_μ) is reconstructed event-by-event at KASCADE-Grande. The procedure involves the maximum log-likelihood technique along with a Lagutin-Raikin distribution function [4].

2.2. Accuracy of EAS Reconstruction

Systematic uncertainties for the core, N_{ch} and arrival direction of the EAS were studied directly [4] by comparing the results of the Grande and KASCADE reconstructions, which work independently, for a subset of data with cores located inside a common area and shower sizes in the interval $\log_{10} N_{ch} = 5.8 - 7.2$. EAS core positions and arrival directions were found to be estimated by Grande with an accuracy of the order of 6 m and 0.8°, respectively. The same evaluation showed that the systematic uncertainties of N_{ch} at Grande are $\leq 5\%$. Those values are in full agreement with expectations from Monte Carlo simulations.

The same kind of study cannot be applied to the muon size since shielded detectors are only available for KASCADE. In this case, Monte Carlo simulations have to be used. The results show that, for $N_{ch} > 10^{4.7}$, the N_μ systematic uncertainties are $\leq 25\%$, decreasing for high energies (see figure 2, left), and exhibit a dependence with the core position and the zenith angle (see, for example, figure 2, right). Since the behavior of the muon uncertainties are well understood, a muon correction function can be constructed and applied to the muon data. This function

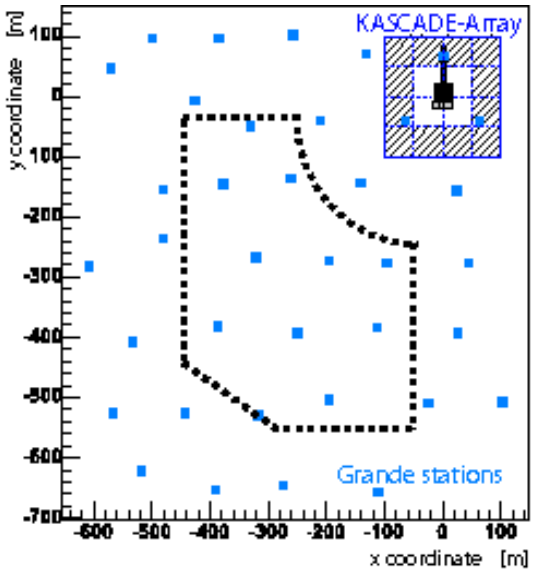

Figure 1: The KASCADE-Grande experiment. Small squares represent the Grande stations. The Kascade array is seen at the upper right hand of the figure. KASCADE detectors are arranged in 16 clusters. The outer 12 clusters contain the muon detectors. The dotted line encloses the fiducial area selected for the present analysis.

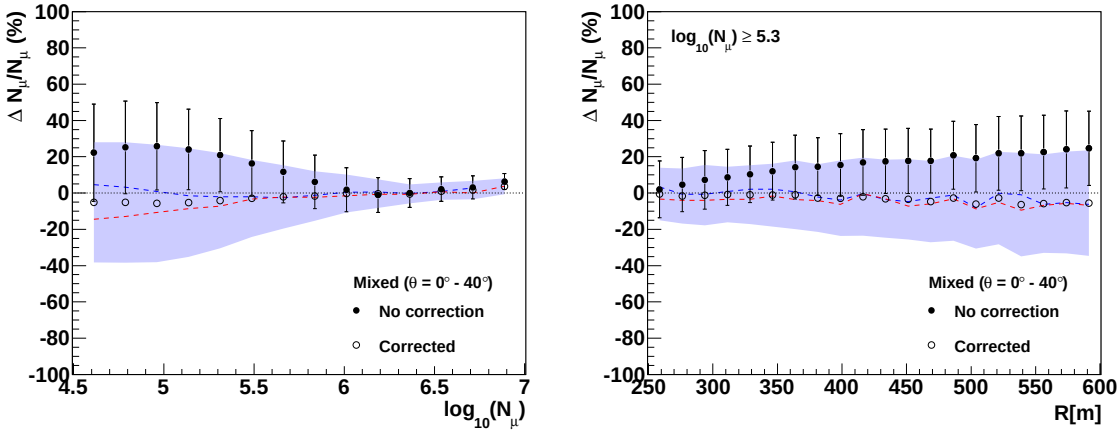

Figure 2: Muon systematic uncertainties vs N_μ (left) and the distance to the KASCADE center (right). The situations before (solid points) and after (open circles) applying the muon correction function are compared. Vertical lines and grey bands represent the one-sigma errors, respectively. Plots were calculated with CORSIKA/QGSJET II for a mixed composition. Dotted lines correspond to pure proton and iron nuclei after using the muon correction function (upper and lower dashed lines, respectively).

was built from Monte Carlo simulations for a mixed composition assumption and was parameterized as a function of the muon size, the EAS arrival direction and the distance to the KASCADE center. The systematic uncertainties of the corrected muon number are $\leq 15\%$ at threshold and quickly decrease for higher muon numbers as seen in figure 2.

3. The energy spectrum

3.1. Data sample

In order to reduce the influence of systematic uncertainties in the data, a fiducial area located at the center of KASCADE-Grande (as shown in figure 1) was selected and only events with zenith angles $\theta \leq 40°$, which passed the KASCADE-Grande reconstruction without failures were considered. Additionally, several experimental cuts were imposed, which results in an effective time of observation of 1173 days and an exposure of $2.003 \cdot 10^{13}\,\mathrm{m}^2 \cdot \mathrm{s} \cdot \mathrm{sr}$. Simulations show that for the above conditions full trigger and reconstruction efficiency at KASCADE-Grande is found above $E \approx 10^{16}\,\mathrm{eV}$.

Simulations were employed to study the systematic uncertainties, the performance and reconstruction methods in the experiment as well as the influence of the cuts. Both the air shower production and development were realized using CORSIKA [6] and the hadronic generators FLUKA [7] and QGSJET II [8]. Events with an homogeneous core distribution and isotropic arrival direction were produced for a $\gamma = -2$ power law spectrum ($E = 10^{15} - 3 \cdot 10^{18}\,\mathrm{eV}$) and sets were generated for a mixed composition of H, He, CO, Si and Fe on similar abundances. A weight function was finally applied to the simulated data to describe a spectrum with $\gamma = -3$, which resembles the observed value.

3.2. Strategy

To reconstruct the energy spectrum, three independent techniques have been applied here: one based solely on the total charged number of particles [9], another one on the muon number [10], and the last one on a combination of both observables [11].

In the ideal case, when the measurements are accurate enough, when the reconstruction procedures work properly, when the Monte Carlo simulations are a faithful description of the EAS and the cosmic ray composition is known one expects the same spectrum from all three methods. But since these conditions are not fulfilled, some differences are expected among the final experimental results. At this point, the present strategy shows different advantages, it allows (1) to carry out different cross-checks of the reconstruction procedures, the influence of systematic uncertainties and the performance of the detectors, (2) to test the sensitivity of N_{ch} and N_μ to the elemental composition and (3) to study the validity of hadronic interaction models. In the next section, the different reconstruction methods and results will be described. It is worth to say that the reconstruction of the energy spectrum has also been performed via the density of carged particles at a distance of 500 m [12], but the results of this study deserves a more detailed discussion. They will be presented in an upcoming paper.

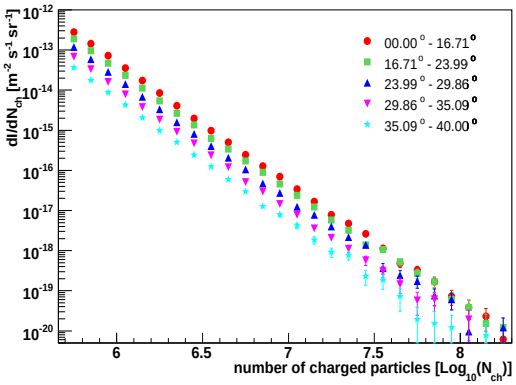

Figure 3: The N_{ch} differential spectra derived from KASCADE-Grande measurements.

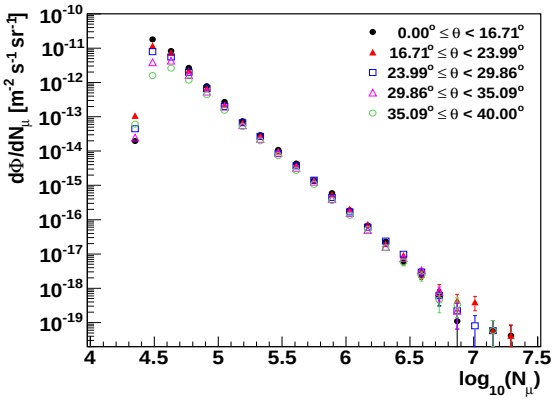

Figure 4: The N_μ differential spectra derived from KASCADE-Grande measurements. The muon correction function was applied to the data.

3.3. Reconstruction with a single observable

The simplest way to reconstruct the energy spectrum is by using one single parameter, as N_{ch} or N_μ [9, 10]. Data is divided in five zenith angle intervals with equal acceptance. In each case, the corresponding shower size spectrum is extracted (see figures 3 and 4) and the constant intensity cut (CIC) method is applied to correct for attenuation effects in the atmosphere. A reference angle, θ_{ref}, must be chosen for this task. In this study, θ_{ref} corresponds to the mean of the corresponding zenith angle distribution, which for N_{ch} is 20° and for N_μ, 22°. The difference comes from the particular cuts applied in each case.

As a next step, from the corrected observable the energy is inferred event-by-event by invoking a Monte Carlo calibration function, which is composition dependent. The calibration formula is obtained by fitting with a power law expression, $E = \alpha \cdot N^{\beta}_{ch(\mu)}$, the Monte Carlo data points for true energy vs shower size around θ_{ref} for different mass groups. Then, all data from the distinct zenith angle intervals is combined according to the energy and a single energy spectrum is obtained.

In a final step, the effect of migration of events in the reconstructed energy spectrum is taken into account by applying a response matrix, R_{ij} (also extracted from simulations). If n_i^{exp} and n_j^{true} are the number of events inside the reconstructed and true energy intervals, $\log_{10} E_i$ and $\log_{10} E_j^{true}$, respectively, then the response matrix is applied in the following way: $n_j^{true} = \sum_{i=1} R_{ij} n_i^{exp}$, where $\sum_{i=1} R_{ij} = 1$, since it represents the $\log_{10} E_j^{true}$ probability distribution of an event with reconstructed energy inside the bin $\log_{10} E_i$. Before unfolding, the response matrix has to be smoothed to avoid the introduction of artificial fluctuations due to the limited statistics in Monte Carlo simulations. In figure 5, the unfolded spectra are plotted.

3.4. $N_{ch} - N_\mu$ method

This path to reconstruct the energy spectrum exploits the information from both the N_{ch} and N_μ observables [11]. The energy of an EAS is derived through a Monte Carlo expression, which involves the values of the total number of charged particles and the muon size in order to reduce the composition dependence of the energy assignment for the EAS. The formula has the form

$$\begin{aligned} \log_{10}(E/GeV) &= [a_p + (a_{Fe} - a_p) \cdot k] \cdot \log_{10}(N_{ch}) \\ &+ [b_p + (b_{Fe} - b_p) \cdot k] \end{aligned} \quad (1)$$

where $k = k(N_{ch}, N_\mu)$ is a mass sensitive parameter defined as

$$k = \frac{\log_{10}(N_{ch}/N_\mu) - \log_{10}(N_{ch}/N_\mu)_p}{\log_{10}(N_{ch}/N_\mu)_{Fe} - \log_{10}(N_{ch}/N_\mu)_p} \quad (2)$$

in such a way that for protons the average value of k is close to zero and approximately one for iron nuclei. The constants (a, b) and (c, d) are obtained from fits to the scatter plots of E vs N_{ch} and N_{ch}/N_μ vs N_{ch}, respectively, and performed in the region of maximum efficiency. To take into account the influence of the atmospheric attenuation in the EAS the above formulas are built for every zenith angle interval and applied accordingly. As it was the case for the single parameter reconstruction, the energy spectrum obtained by the present method is corrected for the effect of the migration of events. The final spectrum is shown in figure 5.

3.5. Flux uncertainties

Each method has its own systematic uncertainties, which were carefully estimated when calculating the

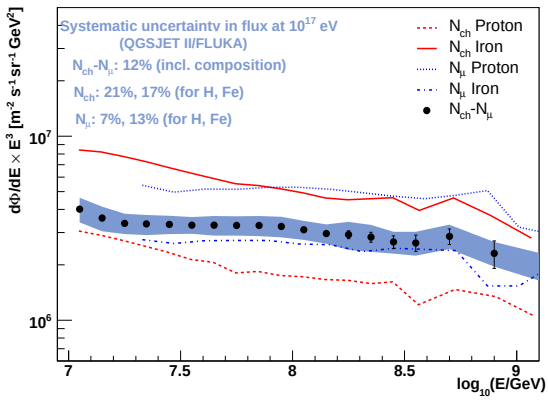

Figure 5: Reconstructed all-particle energy spectrum, multiplied by E^3, as obtained from the KASCADE-Grande data and the different methods described in the present paper. The grey band represents the preliminary systematic uncertainty for the spectrum reconstructed through the $N_{ch} - N_\mu$ method.

energy spectrum. In the case of the single parameter reconstruction the sources of systematic uncertainties considered for this work were the following ones: the energy calibration relation, the CIC method, the muon correction function, the uncertainty of the spectral index and the response matrix. For the $N_{ch} - N_\mu$ method the contributions to the systematic errors of the spectrum come from the atmospheric attenuation, the energy calibration function, uncertainties in the primary composition (applying the method to MC simulations with different composition assumptions), the spectral slope, and the accuracy of the reconstruction of shower sizes. The total systematic uncertainties of the reconstructed spectra at 10^{17} eV for the different methods are shown in figure 5.

4. Discussion

As it was pointed out before, the reconstruction of the energy spectrum by using several methods allows to perform several tests and cross-checks. First, by a direct comparison of the resulting all-particle energy spectra from the KASCADE-Grande data, a good agreement is found inside the respective systematic uncertainties, which means that the experiment and its components are well understood, also that the reconstruction techniques are working as expected and that the hadronic interaction model employed, QGSJET II/FLUKA, is intrinsically consistent.

Another interesting observation from figure 5, it is that the muon size at sea level is a very good and composition independent energy estimator compared with the total number of charged particles. This conclusion is deduced when comparing the difference between the solutions derived from the N_μ method against the one obtained through the N_{ch} approach alone.

Some general insights about the composition of cosmic rays at high energies can also be extracted from these graphs. By departing from the idea that the true energy spectrum should lie inside the solutions obtained from the N_μ and the N_{ch} methods, taking into account that the energy spectrum obtained from N_μ by assuming pure protons (iron nuclei) is higher (lower) than the one derived from N_{ch} and looking at the position of the spectrum from the $N_{ch} - N_\mu$ method, then it is noticed that the common solution spanned by the different methods favors a relatively heavy composition at high energies inside the QGSJET II/FLUKA framework.

To investigate the details of the energy spectrum derived from the $N_{ch} - N_\mu$ approach, a residual plot was constructed by a direct comparison with a flux proportional to $E^{-3.015}$ (see figure 6). The spectral index of the reference flux was obtained by fitting the middle range of the experimental spectrum, i.e. the interval $E = 10^{16.2} - 10^{17}$ eV. Two features shows up at figure 6, one is a concavity above 10^{16} eV and another one is a small break at $\approx 10^{17}$ eV. Both structures are found to be statistically significant. For example, a fit with a power law spectrum above 10^{17} eV gives a spectral index of $\gamma = -3.24 \pm 0.08$. A preliminary statistical analysis with the F-test shows that the significance associated with this change of the spectral index is at a level of $\approx 99.8\%$.

In figure 7, the energy spectrum of cosmic rays obtained from the KASCADE-Grande measurements is compared with the spectra obtained by other cosmic ray instruments. In general, a good agreement is observed at low and high energies with the KASCADE-Grande data.

By now the analysis of the influence of the hadronic

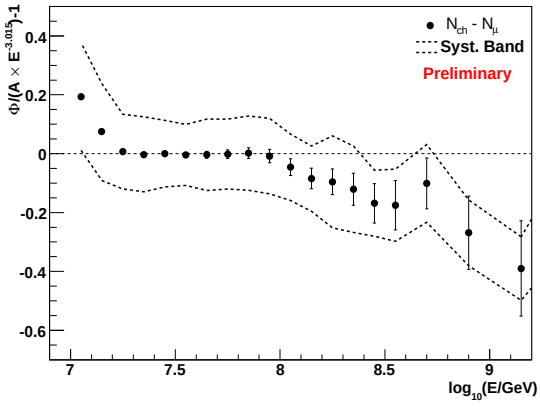

Figure 6: Residual plot for the reconstructed all-particle energy spectrum obtained from KASCADE-Grande through the $N_{ch} - N_\mu$ method. The systematic error band is also shown (dotted lines).

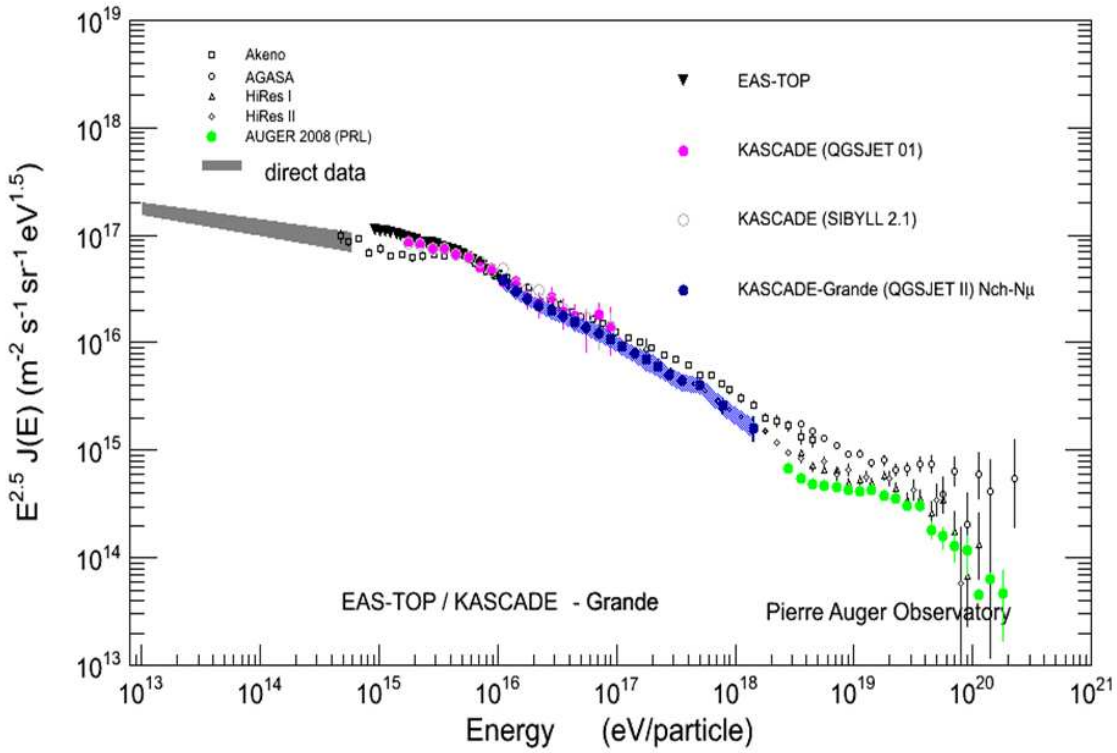

Figure 7: A comparison of the all-particle energy spectrum reconstructed from the KASCADE-Grande data through the $N_{ch} - N_{\mu}$ method with the spectra derived by other experiments.

interaction models is restricted by the statistics of the Monte Carlo data sets generated with alternative hadronic models. However, some preliminary studies applying the reconstruction N_{ch} method [13] and the two-observables approach have been already performed with EPOS v1.99 [14]. Those analysis show that the differences between the reconstructed spectra using EPOS v1.99 and QGSJET II are of the order of $10-15\%$. The same preliminary tests done with EPOS v1.99 also suggest that the observed stuctures at the energy spectrum reconstructed with QGSJET II are not an artifact of the hadronic interaction model.

5. Conclusions

The all-particle energy spectrum of cosmic rays was reconstructed from the KASCADE-Grande data using three different techniques and the hadronic interaction models QGSJET II and FLUKA. The resulting energy spectrum shows statistical significant features that can be identified with a concavity and a small break at $\approx 10^{16}$ and 10^{17} eV, respectively. The nature of this structures are under discussion. Information about the composition in this energy interval will provide valuable clues to solve the mistery. These composition studies are now right underway at KASCADE-Grande.

Acknowledgments

This study was partly supported by the DAAD-Proalmex program (2009-2010). J.C. Arteaga acknowledges the partial support from CONACyT and the Coordinación de la Investigación Científica de la Universidad Michoacana.

References

[1] M. Nagano and A.A. Watson, Rev. Mod. Phys. **72**, 689 (2000).
[2] A. M. Hillas, J. Phys. G: Nucl. Part. Phys. **31**, R95 (2005).
[3] V. Berezinsky *et al.*, Phys. Rev D **D74** (4), 043005 (2006).
[4] W.D. Apel *et al.*, KASCADE-Grande Coll., NIM A **620**, 202 (2010)
[5] T. Antoni *et al.*, KASCADE Coll., NIM A **513**, 490 (2003)
[6] D. Heck *et al.*, Forschungszentrum Karlsruhe, Report FZKA 6019 (1998).
[7] A. Fassò *et al.*, Proc. Monte Carlo 2000 Conf., Lisbon, 955 (2001).
[8] S. S. Ostapchenko, Phys. Rev **D74**, 014026 (2006).
[9] D. Kang *et al.*, KASCADE-Grande Coll., Proc. 31^{st} ICRC, icrc1044, (2009).
[10] J.C. Arteaga *et al.*, KASCADE-Grande Coll., Proc. 31^{st} ICRC, icrc0805, (2009).
[11] M. Bertaina *et al.*, KASCADE-Grande Coll., Proc. 31^{st} ICRC, icrc0323, (2009).
[12] G. Toma *et al.*, KASCADE-Grande Coll., Proc. 31^{st} ICRC, icrc0347, (2009).
[13] D. Kang *et al.*, KASCADE-Grande Coll., these proceedings.
[14] T. Pierog et al., Proc. 31^{st} CIRC, icrc0428, (2009).